ORIGINAL RESEARCH

Shengjie Tongyu Decoction Regulates Cardiomyocyte Autophagy Through Modulating ROS-PI3K/Akt/mTOR Axis by LncRNA H19 in Diabetic Cardiomyopathy

Sixuan Wang, MD; Jun Duan, MD; Jiangquan Liao, MD; Yan Wang, MD; Xiang Xiao, MD; Lin Li, MD; Yi Liu, MD; Huan Gu, MD; Peng Yang, MD; Dongliang Fu, MD; Jinhang Du, MD; Xianglun Li, MD; Mingjing Shao, MD

ABSTRACT

Context • Diabetic cardiomyopathy (DCM) is particularly dangerous in diabetes mellitus (DM). The Shengjie Tongyu decoction (SJTYD) is a well-known, traditional Chinese medicinal formulation that practitioners use to treat myocardial diseases in China; however, its role in DCM remain unclear.

Objective • The study intended to investigate: (1) SJTYD's role in the treatment of DCM and its underlying mechanisms, (2) the association of autophagy with DCM, and (3) the involvement of mammalian target of rapamycin (mTOR) signaling in the regulation of DCM.

Design • The research team performed an animal study.

Setting • The study took place in the Department of Endocrinology in the No. 2 ward—Traditional and Complementary Medicine(TCM) of the China-Japan Friendship Hospital in Beijing, China.

Animals • The animals were 60 C57/BL6 mice weighing 200-250 g.

Intervention • To determine the role of SJTYD in treating DCM, the research team established a mouse model of DM using streptozotocin (STZ). The team randomly divided the mice into three groups with 20 mice each: (1) a negative control group, which didn't receive injections of STZ or treatment with SJTYD; (2) a model group, the Model group, which received injections of STZ but didn't receive treatment with SJTYD; and (3) an SJTYD group, which received injections of STZ and treatment with SJTYD.

Outcome Measures • The research team: (1) conducted a differential analysis to identify the differentially expressed genes; (2) performed deep sequencing of the long noncoding RNAs (lncRNAs) expressed in cardiomyocytes from the control, Model, and SJTYD groups; (3) performed a bioinformatics analysis; (4) used the ultrasonic and pathological, transmission electron microscopy (TEM) test as well as a Western blot to evaluate cardiac function, myocardial-injury areas, and autophagy in vivo; (5) transfected primary cardiomyocytes treated them with lncRNA H19 and SJTY 3-MA to establish SJTYD subgroups in which the H19 protected against DCM and the 3-MA inhibited autophagy; and (6) carried out immunofluorescence staining and Western blot to test the phosphorylated levels of phosphoinositide 3-kinase (PI3K)/ protein kinase B (AKT)/ mammalian target of rapamycin (mTOR) as well as autophagy levels in vitro.

Results • The bioinformatics analysis indicated that SJTYD significantly modulated lncRNA H19 as well as the mTOR pathway. The vevo2100's results indicated the SJTYD reversed the cardiac-dysfunction parameters in DCM. The Masson' staining, TEM, and Western blot demonstrated that the SJTYD could suppress the myocardial-injury areas as well as the numbers of autophagosomes and the expression proteins of autophagy in vivo. The SJTYD promoted the phosphorylated-levels of PI3K, AKT, and mTOR and decreased the levels of autophagy proteins. LC3A-II and Beclin-1; lncRNA H19 amplified the SJTYD's role; and 3-MA reversed those effects, as tested using immunofluorescence and Western blot in primary cardiomyocytes.

Conclusions • The SJTYD can protect against diabetic myocardial injury by inhibiting cardiomyocyte autophagy through the activation of lncRNA H19, reactive oxygen species (ROS), and the PI3K/Akt/mTOR signaling pathway. SJTYD may be an effective strategy to ameliorate diabetic myocardial injuries. (*Altern Ther Health Med.* 2023;29(6):280-287).

Sixuan Wang, MD, physician, and **Jun Duan,** MD, physician, Department of Endocrinology, No. 2 ward—Traditional and Complementary Medicine(TCM), China-Japan Friendship Hospital, Beijing, China. **Jiangquan Liao,** MD, physician; **Yan Wang,** MD, Physician; **Xiang Xiao,** MD, physician; **Lin Li,** MD, physician; **Yi Liu,** MD, Physician; **Huan Gu,** MD, physician; **Peng Yang,** MD, chief physician; **Dongliang Fu,** MD, physician; **Jinhang Du,** MD, Physician; **Xianglun Li,** MD, Physician; and **Mingjing Shao,** MD, Physician; National Integrated Traditional and Western Medicine Center for Cardiovascular Disease, China-Japan Friendship Hospital, Beijing, China

Corresponding author: Xianglun Li, MD
E-mail: lixianlun@hotmail.com

Diabetes mellitus (DM) is a major, worldwide health problem that has a high mortality rate due to many severe complications.[1] Among them, diabetic cardiomyopathy (DCM) is particularly dangerous.[2,3] DCM refers to damage to myocardial structure and function resulting from DM, and its significant features include ventricular hypertrophy, myocardial fibrosis, ventricular dilation, and cardiomyocyte damage or death, thus resulting in cardiac dysfunction and progression to cardiac arrhythmia, heart failure, or even cardiogenic death.[4-7] Therefore, the importance of treatment for DCM can't be overstated.

Pathophysiological Mechanisms

At present, scientists consider oxidative stress, metabolic abnormalities, and cell death to be DCM's fundamental pathophysiological mechanisms. Generally, metabolic dysfunction that high glucose induces and that leads to cardiomyocyte destruction is consistent with elevated oxidative stress as well as cell apoptotic or death markers.[8]

Only with an improved understanding of DCM's mechanisms can researchers develop new therapies to reduce the risk of disease progression. Therefore, it's urgent to perform experimental studies on the control and therapeutic targets of DCM.

Some studies have demonstrated that lncRNAs can play a role in multiple physiological processes associated with the pathophysiology of numerous cardiovascular disorders, including DCM.[9-11] Long noncoding RNAs (lncRNAs) are RNA transcripts that are >200 nucleotides in length and that lack protein-coding potential.[9] The H19 gene, which is crucial in DCM, is a maternally expressed gene that encodes lncRNA 19—a 2.3-kb non-coding RNA—and is conserved in evolution.[12-15]

Autophagy

Autophagy is a catabolic process that can degrade and recycle cellular components and damaged organelles in various diseases. It's a key metabolic process that protects cellular homeostasis by eliminating many superfluous or dysfunctional cellular elements in a lysosome-dependent way.[16,17] The dysregulation of autophagy can induce many human disorders, such as cardiovascular diseases.[18,19]

Scientists generally consider oxidative stress to be an important intracellular signal transducer for sustaining autophagy. At an early stage, autophagy primarily behaves as a pro-survival mechanism for cellular survival. However, autophagy can contribute to cell-death processes when facing sustained reactive oxygen species (ROS). Yun et al found that the excessive production of ROS can cause oxidative damage and cellular death,[20] which Mehrzadi et al and Muriach et al found could occur under pathological conditions.[21,22]

A consensus exists that cardiomyocyte inflammation, disorders of the mammalian target of rapamycin (mTOR)-related signaling pathway, and myocardial-autophagy imbalance can lead to cardiomyocyte damage and a decline in cardiac function in the context of high glucose levels.[23] Two previous studies found that activation of phosphoinositide 3-kinase (PI3K), protein kinase B Akt, and mTOR can suppress oxidative stress by elevating the expression of nuclear respiratory factor (Nrf), the major inhibitor for ROS, and inhibiting autophagy.[24,25] The pro-survival kinases PI3K and Akt can activate mTOR.[26,27]

In high-glucose or diabetic environments, ROS can generate nicotinamide adenine dinucleotide phosphate (NADPH) oxidases (NOX), such as NOX2 and NOX4, which are indispensable for the recruitment of LC3B.[28] This facilitates conversion of LC3B-I to the conjugate LC3B-II 33 and activation of various autophagy-related (ATG) proteins, such as Beclin-1, ATG5, and ATG7,[29] and eventually results in autophagy. Therefore, medical practitioners should use anti-autophagy treatment for DCM.

Traditional Chinese Medicine (TCM)

In TCM, practitioners think that the basic pathogenesis of cardiovascular disease is stagnation of qi and blood stasis and homeostatic imbalance; therefore, clinicians often use the method of promoting blood circulation and removing blood stasis to help cure cardiovascular diseases.[30,31]

TCM's Shengjie Tongyu decoction (SJTYD) consists of Radix Astragali seu Hedysari, Radix Platycodonis, Radix Bupleuri, Rhizoma Anemarrhenae, Fructus Corni, Rhizoma Sparganii, Rhizoma Cimicifugae, and Herba Leonuri; practitioners have used it to treat myocardial diseases for a long time, and it has achieved significant efficacy in China.[32]

Three previous studies have shown that SJTYD can exert anti-oxidant properties, which may be powerfully useful for treating DCM.[33-35] However, no research has occurred to study the effects of SJTYD in treating DCM.

Current Study

The current study intended to investigate: (1) SJTYD's role in the treatment of DCM and its underlying mechanism, (2) the association of autophagy with DCM, and (3) the involvement of mammalian target of rapamycin (mTOR) signaling in the regulation of DCM.

METHODS

Animals

The research team performed an animal study, which took place in the Department of Endocrinology in the No. 2 ward—Traditional and Complementary Medicine(TCM) of the China-Japan Friendship Hospital in Beijing, China.

The research team purchased C57/BL6 mice weighing 200-250 g from Beijing Haidian Xinglong Experimental Animal Center (Beijing, China) and housed them for two weeks under a 12-h light/dark cycle at room temperature, providing them with an initial high-sugar, high-fat feed before the study.Cardiomyocytes are taken after grouping.

The Laboratory Animal Ethical Committee of the China-Japan Friendship Hospital reviewed and approved the animal-use protocol for this study (No. zryhyy 61-22-04-05).

Procedures

Drugs and reagents. The research team purchased the SJTYD formulation from the Department of Traditional Chinese Medicine at China-Japan Friendship Hospital. The formulation comprised Radix Astragali seu Hedysari, Radix Platycodonis, Radix Bupleuri, Rhizoma Cimicifugae, and Herba Leonuri. The team mixed the herbal liquid with a Radix Ginseng decoction and decocted it with water for 1.5 h.

DM Model. To determine the role of SJTYD in treating DCM, the research team established a mouse model of DM as Thomas et al previously described.[3] The research team randomly divided the mice into three groups with 20 mice each: (1) a control group, which didn't receive injections of streptozotocin (STZ) or treatment with SJTYD; (2) a model group, the Model group, which received injections of STZ but didn't receive treatment with SJTYD; and (3) an SJTYD group, which received injections of STZ and treatment with SJTYD.

The team suspended the STZ from Sigma-Aldrich (Shanghai, China) in a citrate buffer at pH 4.2, mitigated it with 0.9% NaCl saline (Baxter, Shanghai, China), and dispensed it intraperitoneally at a dose of 50 mg/kg/day. The team injected the Model and SJTYD groups with STZ for 4 days and collected fasting venous blood from each mouse to measure the development of DM. A blood-glucose level of higher than 16 mM indicated DM, whereas a level less than 7 mM indicated no DM.

The team: (1) administered SJTYD to the SJTYD group by gavage daily for 4 weeks; (2) used Vevo2100 VisualSonics (VisualSonics, Shanghai, China) for testing the myocardial functions of the mice; and (3) measured the left ventricular (LV) pressure using a micromanometer-tipped catheter (Millar, Texas, USA) in the LV and then recorded the ejection fraction (EF) and fraction shortening (FS), the left ventricular systolic (LV Vol;s) and diastolic (LV Vol;d) volumes.

Cardiomyocyte culture. The research team: (1) isolated ventricular myocytes from the mice , as Liu et al described earlier[15]; (2) briefly carried out a thoracotomy after deeply anesthetizing and sacrificing the mice using intracardiac perfusion with ketamine (90 mg/kg); (3) harvested the hearts and crushed them in Hanks' solution (Sigma-Aldrich, Shanghai, China), a balanced salt solution that is free of Ca2+ and Mg2+; (4) incubated the tissues at 37°C in D-Hanks solution containing 3 μM of Mito-SOX Red (Invitrogen, Carlsbad, CA, USA).

The team then: (1) suspended the cells after centrifugation in high-glucose Dulbecco's Modified Essential Medium (Gibco, Paisley, UK), supplemented with 10% heat-inactivated fetal calf serum, 12.5 mM sodium [N-(2-hydroxyethyl) piperazine-N'-(2-ethanesulfonic acid)] (HEPES) with pH 7.3, and 0.1 mM bromodeoxyuridine and (2) incubated the cardiomyocytes at room temperature in a humidified chamber.

RNA extraction, library preparation, and sequencing. The research team: (1) extracted total RNA from myocardial tissues and cultured cardiomyocytes using TRIzol reagent (Invitrogen,), according to the manufacturer's instructions; (2) verified total RNA integrity and purity using formaldehyde-agarose-gel electrophoresis using equipment from Thermo Fisher (Shanghai, China) and an OD260/280 ratio of >1.85; (3) prepared the rRNA-depleted sequencing libraries from total RNA using the Illumina TruSeq Stranded Total RNA Gold (Illumina,Santiago, California, USA); and (4) used a quantity of total RNA, about 1 μg, as input material and removed both cytoplasmic and mitochondrial rRNAs using a Ribo-Zero Gold kit (Illumina, Santiago, California, USA).

The team then: (1) performed RNA purification, reverse transcription, library construction, and sequencing using a kit from Guangzhou RiboBio (Guangdong, China), according to the manufacturer's instructions (Illumina); (2) after library construction, used the Qubit dsDNA HS Assay (Thermo Fisher Scientific, Shanghai, China) to quantify the concentration of the resulting sequencing libraries; (3) analyzed the size distribution using an Agilent 2100 Bioanalyzer. (Agilent, Santa Clara, California, USA); and (4) performed sequencing using an Illumina system, following Illumina's provided protocols for 2 x 150 paired-end sequencing, at RiboBio.

LncRNA-expression estimation and differential-expression analysis. The research team: (1) trimmed raw reads with Fastp, v0.2.2 (Hyplos, Shenzhen, China) to remove adapter sequences and low-quality bases; (2) aligned the clean reads to the referenced human genome GRCh37/hg19 with STAR, v2.4.2a (Illumina, Santiago, California, USA)[37]; and (3) used RNA-Seq by Expectation-Maximization (RSEM)[38] from Bioconda (USA) to estimate gene abundance based on the uniquely mapped reads.

The team then: (1) used the genome research part of the ENCyclopedia of DNA Elements (ENCODE) scale, GENCODE, v19, to annotate mRNAs and lncRNAs in the above process; and (2) used the edgeR package[39] (USA) to identify differentially expressed genes (DEGs) and set the screening criteria for DEGs to [log2(fold change)] >2 and an adjusted $P < .05$.[40]

Functional enrichment analysis. The research team: (1) subjected the identified differentially expressed lncRNAs/messenger RNAs (mRNAs) of the control, Model, and SJTYD groups to pathway analyses using Gene Ontology (GO)[41] and the Kyoto Encyclopedia of Genes and Genomes (KEGG)[41] to identify the significant pathways associated with differentially expressed lncRNAs and (2) conducted a Fisher's exact test (Cochran's restriction) to select the significant pathways. $P < .05$ indicated statistical significance.

Transfection and generation of stably transfected cardiomyocyte lines. The research team: (1) purchased the full-length, lncRNA H19, overexpression sequence si-H19 from GenePharma (Shanghai, China); (2) mixed the transfection reagent Lipofectamine 3000 (Invitrogen) and plasmids, including si-H19, and added them to cardiomyocytes with the medium for 5 h, followed by transfection in a regular, serum-containing medium for another day; and (3) collected the cells for the detection of mRNA levels using a real-time quantitative polymerase chain reaction (RT-qPCR).

RT-qPCR. The research team: (1) extracted total RNA from heart tissues and cardiomyocytes using TRIzol reagent

(Invitrogen); (2) synthesized complementary deoxyribose nucleic acid (cDNA) using a RT-qPCR kit (Invitrogen), according to the manufacturer's instructions; (3) performed the RT-qPCR using the SYBR Green Real-time PCR Master Mix (Toyobo, Osaka, Japan) with a 7500 Fast Real-Time PCR System (Applied Biosystems, Carlsbad, California, USA). The primer sequences (5'-3') were as follows: H19: 5'-TATCGGAC TCCAGAGGGATT-3' and 5'-GGCATACAGTGCACCA AGTC-3'. The team calculated the relative expression level of genes using the 2−ΔΔCT method.

Western blotting. The research team: (1) homogenized the tissues in 0.1% sodium dodecyl sulfate (SDS) buffer, which contained 0.05 M of sodium chloride (NaCl), 10 mM of ethylenediaminetetraacetic acid (EDTA), 25 mM of sodium HEPES, 10 mM of sodium orthovanadate (Na_3VO_4), 1 mM of dithiothreitol (DTT), 20% glycerol, and 1.0% Triton X-100, supplemented with protease inhibitor cocktail (Complete TM mini, Boehringer-Mannheim, (Mannheim, Baden-Wurttemberg, Germany); (2) centrifuged the lysate at 12 000 rpm for 15 min and harvested the supernatant containing the cytoplasmic proteins and measured them using the RC DC Protein Assay Kit (Bio-Rad, Hercules, CA, USA); (3) separated 50 μg of the extracted protein using equipment for sodium dodecyl-sulfate polyacrylamide gel electrophoresis (SDS-PAGE) from Thermo Fisher (Shanghai, China) and transferred it onto a polyvinylidene fluoride (PVDF) membrane (Millipore, Bedford, MA, USA).

The team then: (1) blocked the membrane with 3% bovine serum albumin (BSA) and phosphate-buffered saline (PBS) for one h to reduce nonspecific antibody binding; (2) incubated the membrane with the primary antibody Atg-5, beclin-1, LC-3II, p-PI3K, t-PI3K, p-AKT, t-AKT, p-mTOR, LC3B and GAPDH(1:1000, Abcam, UK) at 1:100 in PBS for 12 h at room temperature; (3) incubated it again with Goat anti-rabbit IgG H&L (HRP) pre-adsorbed secondary antibody(1:5000, Abcam, UK) for 40 min at room temperature; and (4) detected the signal using an enhanced chemiluminescence (ECL) system (Amersham Biosciences, Little Chalfont, UK) and exposed it to X-ray films.

Transmission electron microscopy (TEM). The research team: (1) sliced sample tissues into three minor sections, fixed them in 2.5% glutaraldehyde, then fixed them in 1% osmium tetroxide, and embedded them in epoxy resin overnight and (2) stained the sections with uranyl acetate for 30 min and lead citrate for 5 min and observed them under a Philips CM120 model transmission electron microscope (Philips, Amsterdam, Netherlands).

Masson's staining. After fixing tissues in 10% buffered formalin for at least 24 h at room temperature, the research team embedded 4-mm sections in paraffin and then stained them with Masson's trichrome (MKbio, Shanghai, China) to investigate the fibrotic changes.

Immunofluorescence. The research team: (1) plated cells on coverslips in a 24-well plate; (2) fixed them with paraformaldehyde for 15 min and permeated them with PBST—0.1% Triton X-100 in D-PBSA—for 25 min; (2) after blocking them with 5% normal goat serum for 40 min at room temperature, incubated the cells overnight at 4°C with phosphorylated (p)-mTOR Ser2448 primary antibodies (Cell Signaling Technology, Boston,USA); and (3) observed them under a fluorescent microscope, an Olympus BX51 (FULAI OPTICAL TECHNOLOGY, Shanghai,China) and analyzed the images with ImageJ software (NIH) (Bethesda, Maryland, USA).

Outcome measures. The research team: (1) conducted a differential analysis to identify the differentially expressed genes; (2) performed deep sequencing of the long noncoding RNAs (lncRNAs) expressed in cardiomyocytes from the control, Model, and SJTYD groups; (3) performed a bioinformatics analysis; (4) used the ultrasonic and pathological TEM test as well as a Western blot to evaluate cardiac function, myocardial-injury areas, and autophagy in vivo; (5) transfected primary cardiomyocytes treated them with lncRNA H19 and SJTY 3-MA to establish SJTYD subgroups in which the H19 protected against DCM and the 3-MA inhibited autophagy; and (6) carried out immunofluorescence staining and Western blot to test the phosphorylated levels of phosphoinositide 3-kinase (PI3K)/ protein kinase B (AKT)/ mammalian target of rapamycin (mTOR) as well as autophagy levels in vitro.

Outcome Measures

Cardiac functions. The research team carried out hemodynamic measurements to assess the cardiac systolic and diastolic functions of the mice.

Myocardial injury. The research team examined the degree of myocardial injury in each group, so that further investigation of the effects of SJTYD in treating DCM could occur.

lncRNA H19 in cardiomyocytes. To obtain an intensive understanding of the mechanism by which H19 protects against DCM, the research team extracted RNA from the peripheral blood of the Model and SJTYD groups, followed by RNA-seq analysis. In consideration of the gene function in enriched pathways, the research team selected lncRNA H19, an lncRNA related to apoptosis and autophagy signaling pathways.

To explore the functional pathways that SJTYD influences, the research team conducted pathway analyses and compared the DCM and SJTYD groups. Considering the enriched pathways and their roles in DCM, the team selected the downregulated pathways for further investigation, including autophagy, flavonoid glucuronidation, flavonoid biosynthetic process, and endosomal transport. The team chose autophagy-related pathways to explore the correlations between SJTYD and cell death and DCM. In consideration of gene function in enriched pathways, the team selected lncRNA H19, an lncRNA related to apoptosis and the autophagy signaling pathway.

Suppression of cardiomyocyte autophagy. The research team evaluated cardiomyocyte autophagy using 3-MA. The team inspected autophagosomes using TEM and measured the autophagy and associated protein-expression profiles.

PI3K/Akt/mTOR signaling pathway. To determine whether H19 is involved in repressing cardiomyocyte

Figure 1. SJTYD and Cardiac Functions in Diabetic Mice Postintervention (N = 24, 8 in each group). Figure 1A shows representative, serial M-mode echocardiography in the SJTYD, DM (model), and control groups. Hemodynamic measurements revealed that the cardiac systolic and diastolic functions improved in the SJTYD group. The quantitative analysis in Figure 1B shows the SJTYD group's LVEF, LVFS, LV Vol;s and LV Vol;d.

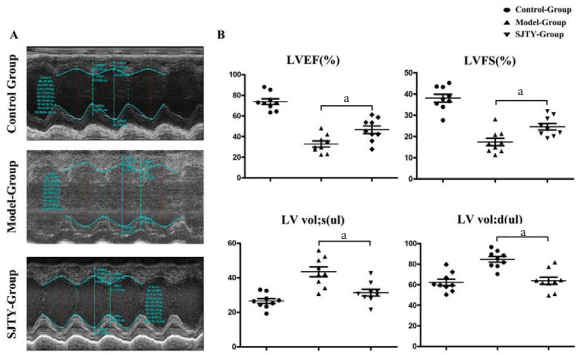

[a]$P < .01$, indicating that the SJTYD group's LVEF and LVFS were significantly higher and its LV Vol;s and LV Vol;d were significantly lower than those of the Model group postintervention

Abbreviations: DM, diabetes mellitus; LVEF, left ventricular ejection fraction; LVFS, left ventricular fraction shortening; LV Vol;d, left ventricular diastolic volume; LV Vol;s, left ventricular systolic volume; SJTYD, Shengjie Tongyu decoction.

Figure 2. SJTYD and Relief of Myocardial Injury in Diabetic Mice Postintervention (N = 24, 8 in each group). Figure 2A shows a photomicrograph of heart tissues stained with modified Masson's trichrome staining, 40×, which revealed that the SJTYD group's myocardial-injury area was smaller than that of the DM (model) group. Figure 2B shows the quantitative analysis of the SJTYD group's and DM (model) group's myocardial-injury areas. Scale bars: 500 μm. Data are means ± SDs.

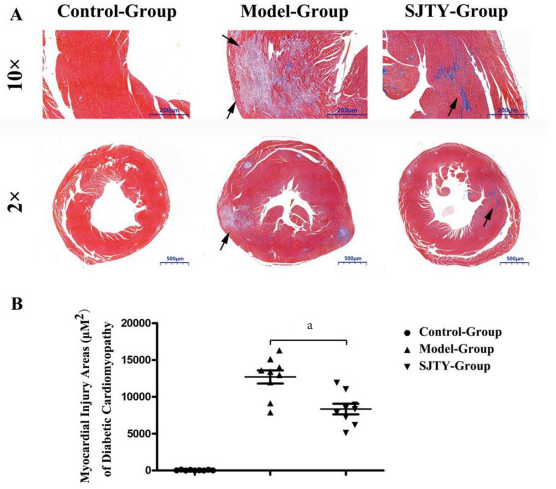

[a]$P < .01$, indicating that the SJTYD group's myocardial-injury area was significantly smaller than that of the Model group postintervention

Abbreviations: SJTYD, Shengjie Tongyu decoction.

autophagy, the research team assessed expression of mTOR, the primary regulator of autophagy. To further determine whether the PI3K/Akt/mTOR signaling pathway is involved in H19-induced cardiomyocyte autophagy, the team injected 3-methyladenine (3-MA), an autophagy inhibitor, into the culture medium of cardiomyocytes.

Statistical Analysis

The research team analyzed the data use SPSS 20.00 software (IBM, New York, USA). The team expressed measurement data as means ± standard deviations (SDs), used Student's *t* test for comparison between groups, and used an analysis of variance (ANOVA) for comparisons between baseline and postintervention. $P < .05$ indicated statistical significance.

RESULTS

Cardiac Functions

Ultrasound experiments (experiments with different interventions at fixed time points) after four weeks of continuous incubation. The SJTYD group's cardiac functions had improved postintervention (Figure 1A). For the quantitative analysis, Figure 1B shows that the group's left ventricular ejection fraction (LVEF) and left ventricular fraction shortening (LVFS) were significantly higher and its left ventricular systolic volume (LV Vol;s) and left ventricular diastolic volume (LV Vol;d) were significantly lower than those of the Model group postintervention (all $P < .05$). These results imply that SJTYD can improve cardiac functions in diabetic mice.

Myocardial Injury

In Figure 2A, the photomicrograph of heart tissues shows that postintervention the SJTYD group's myocardial-injury area was smaller than that of the Model group, suggesting that SJTYD can relieve myocardial injury in diabetic mice. Moreover, the quantitative analysis in Figure 2B shows that postintervention the SJTYD group's myocardial-injury area was significantly smaller than that of the Model group, indicating its protection against DCM development ($P < .05$).

lncRNA H19 in Cardiomyocytes

The analysis found 105 differentially expressed lncRNAs with a fold-change >2.0 and an adjusted $P < .05$, including 60 downregulated ones and 45 upregulated ones (Figure 3A). The LncRNA H19 was significantly upregulated in DM. Figure 3B shows that the lncRNA H19 in the Model and SJTYD groups

Figure 3. RNA-seq Analysis: Protective Effect of H19 after SJTYD Administration (N = 24, 8 in each group). Figure 3A shows the Volcano plot, which exhibited the differentially expressed mRNAs/lncRNAs; Figure 3B shows the expression of lncRNA-H19, according to the RT-qPCR; and Figure 3C shows the LncRNA H19 in cardiomyocytes after SJTYD administration. Figure 3D shows the Kaplan-Meier survival analysis of the expression of the relationship between lncRNA H19 and survival rate. Figure 3E shows the functional enrichment analyses (GO terms) of downregulated enriched pathways, and Figure 3F shows the functional enrichment analyses (GO terms) of upregulated enriched pathways. Figure 3G shows that H19 was positively associated with mTOR in the co-expression analysis ($P < .05$). Data are expressed as means ± SD.

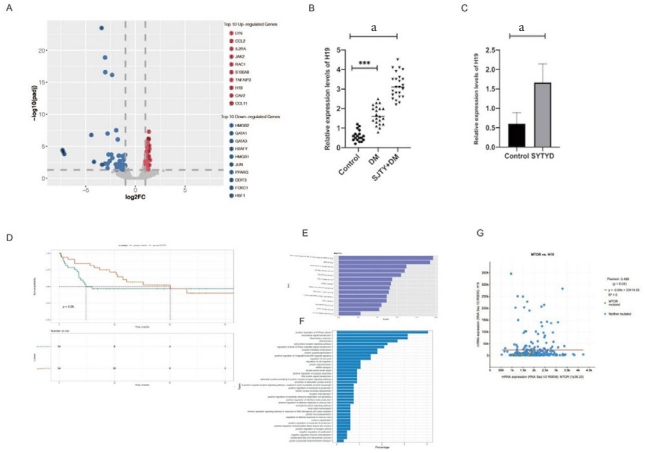

[a]$P < .001$, indicating that mice with a high expression of lncRNA H19 had a significantly higher survival rate than those with a low expression of lncRNA H19

Abbreviations: DM, diabetes mellitus; GO, Gene Ontology; lncRNA H19, long noncoding RNAs; mRNAs, messenger RNA; mTOR, mammalian target of rapamycin; RT-qPCR, real-time quantitative polymerase chain reaction; SJTYD, Shengjie Tongyu decoction.

Figure 4. H19 Gene and Suppression of Cardiomyocyte Autophagy (N = 24, 8 in each group). The image above is an image magnified by 30 000 times, and the image below is magnified by 10 000 times.Figure 4A shows the evaluation of cardiomyocyte autophagy by observation of autophagosomes using TEM. Figure 4B shows the detection of the expression of autophagy-related proteins—LC3A-II, Beclin-1, and ATG5—using Western blotting and quantitative analysis. Scale bars: 500 μm.

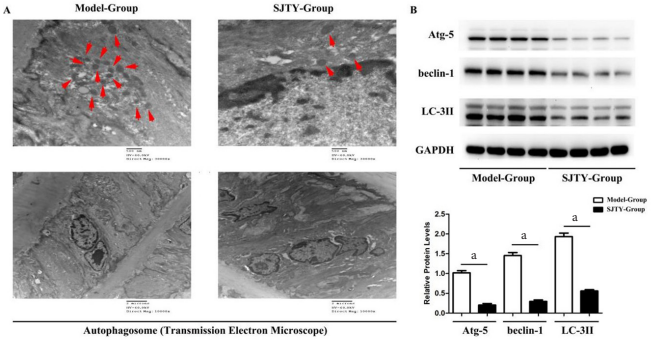

**$P < .01$, indicating that the SJTYD group's number of autophagosomes and its expression of the autophagic markers LC3A-II, Beclin-1, and ATG5 were significantly lower than those of the Model group postintervention

Abbreviations: ATG5, autophagy related 5; LC3-II, Microtubule-associated protein 1A/1B-light chain 3-II; SJTYD, Shengjie Tongyu decoction; TEM, transmission electron microscopy

was significantly higher than that of the control group postintervention (both $P < .01$). Figure 3C shows that the SJTYD group's expression level of lnc RNA H19 was significantly higher in cardiomyocytes postintervention than the control group's was ($P < .01$). Moreover, Figure 3D shows that that mice with a high expression of lncRNA H19 had a significantly higher survival rate than those with a low expression of lncRNA H19 ($P < .001$).

The analysis identified 19 downregulated pathways (Figure 3E) and 38 upregulated pathways (Figure 3F). Figure 3G shows that H19 was significantly positively associated with mTOR ($P < .05$).

Suppression of Cardiomyocyte Autophagy

The Model group's H19 expression in cardiomyocytes was lower than that of the SJTYD group and was higher following injection with H19. The SJTYD group's autophagy was repressed.The image above is an image magnified by 30 000 times, and the image below is magnified by 10 000 times. (Figure 4A).

Western blotting and quantitative analysis (Figure 4B) revealed that postintervention the SJTYD group's number of autophagosomes was significantly lower than that of the Model group ($P < .05$) and its expression of the autophagic markers LC3A-II, Beclin-1, and ATG5 were significantly lower than those of the Model group postintervention ($P < .05$), signifying that H19 is involved in the suppression of cardiomyocyte autophagy.

Hi PI3K/Akt/mTOR Signaling Pathway

The immunofluorescence staining showed that the SJTYD + H19 group's expression of p-mTOR had increased in the cardiomyocytes, suggesting that H19 can reinforce mTOR recruitment in SJTYD (Figure 5A).

Figure 5. H19 and High-glucose-induced Autophagy by Regulating PI3K/Akt/mTOR Signaling Pathway (N = 9, 3 in each group). Figure 5A shows that immunofluorescence revealed an increased expression of p-mTOR in cardiomyocytes of neonatal mice in the SJTYD group. Figure 5B shows that the activity of p-PI3K, p-Akt, and p-mTOR and the expression of autophagy-related proteins— MAP1LC3A-II (LC3A-II), Beclin-1, and ATG5—as detected using Western blotting with and without 3-MA. Scale bars: 20 μm.

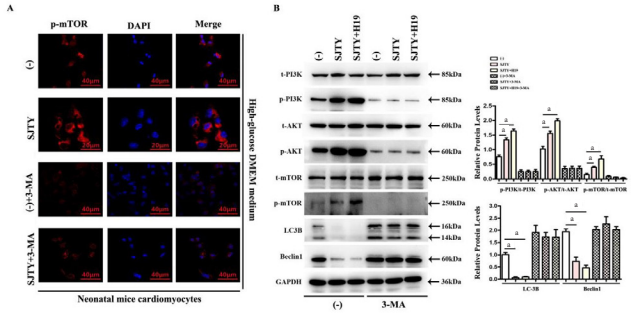

[a]$P < .01$, indicating that the relative protein expressions of p-mTOR, p-PI3K and p-Akt were significantly higher in the cardiomyocytes of the SJTYD + H19 group than in the other groups and were significantly lower for the SJTYD + H19 + 3-MA group than for the other groups

Abbreviations: Akt, protein kinase B; ATG5, autophagy related 5; LC3A-II, Microtubule-associated protein 1A/1B-light chain 3-II; mTOR, mammalian target of rapamycin; PI3K, phosphoinositide 3-kinase; SJTYD, Shengjie Tongyu decoction.

The Western blotting in Figure 5B shows that H19 increased the activity of the p-pro-survival kinases p-PI3, p-Akt, and p-mTOR in cardiomyocytes in response to SJTYD + H19 (Figure 5B).

Furthermore, the quantitative analysis confirmed that the relative protein expressions of p-mTOR, p-PI3K and p-Akt were significantly higher in the cardiomyocytes of the SJTYD + H19 group than control group and SJTYD group ($P < .01$), suggesting that mTOR is activated and positively associated with H19-induced cardiomyocyte autophagy.

Interestingly, the 3-MA significantly reversed the increases in mTOR, p-mTOR, p-PI3K, and p-Akt in cardiomyocytes in the SJTYD + H19 group (Figure 5B), indicating that H19 is involved in cardiomyocyte autophagy that high glucose induces, by regulating the PI3K/Akt/mTOR signaling pathway.

In addition, the quantitative analysis in Figure 5B shows that the relative protein expressions of p-mTOR, p-PI3K, and p-Akt were significantly lower in the SJTYD + H19 + 3-MA group than in control group, SJTYD group and SJTYD + H19 group ($P < .01$). These results imply that mTOR is activated and positively associated with H19, which is involved in the autophagy that high glucose induces, by regulating the PI3K/Akt/mTOR signaling pathway.

DISCUSSION

SJTYD is a kind of traditional Chinese medicine soup, which has the effect of invigorating qi and raising yang, activating blood circulation and removing stasis. In China, it has been used to treat heart failure caused by a variety of diseases, especially in the recovery period after myocardial infarction.[33,35] On this basis, this study aims to explore the pharmacodynamic effect of SJTYD on myocardial infarction, explore its potential mechanism, and explore the potential role of SJTYD in myocardial infarction by constructing a mouse myocardial infarction model.

The ultrasound study found that SJTYD can ameliorate cardiac systolic and diastolic dysfunction, indicating that SJTYD may help to prevent DCM. Furthermore, Masson's staining revealed that the myocardial-injury area was significantly larger in the Model group than in the SJTYD group, suggesting the ability of SJTYD to relieve myocardial injury in diabetic mice.

The current study also found that LncRNA H19 was significantly higher in the Model and SJTYD groups than in the control group. Also, the SJTYD group's expression level of lncRNA H19 in cardiomyocytes was significantly higher than that of the control group.

Moreover, the survival analysis found that the mice with a high expression of lncRNA H19 had a higher survival rate than those with a low expression of lncRNA H19. Pathway analyses between DCM and SJTYD groups showed 19 downregulated pathways and 38 upregulated pathways and co-expression analysis showed that H19 was significantly positively associated with mTOR.

Autophagy means autophagy, which is the process by which eukaryotic cells use lysosomes to degrade their own cytoplasmic proteins and damaged organelles under the regulation of autophagy-related genes. Autophagy prevents cell damage, promotes cell survival in the event of nutrient deficiencies, and responds to cytotoxic stimuli. Autophagy includes basal autophagy under physiological conditions and induced autophagy under stress conditions.[42] SJTYD improved cardiac function and cardiomyocyte structure, signifying its powerful therapeutic effect. The SJTYD group's autophagy and the number of autophagosomes and expression of the autophagic markers LC3A-II, Beclin-1, and ATG7 were significantly lower than those of the Model group, indicating the role of SJTYD in the suppression of cardiomyocyte autophagy. The H19 increased mTOR activity and the SJTYD group's p-mTOR expression in cardiomyocytes was significantly higher than that of the DCM group, suggesting that mTOR is activated and positively associated with H19-induced cardiomyocyte autophagy. The Western blotting showed that H19 increased p-PI3K and p-Akt in cardiomyocytes in the SJTYD group.

To further determine whether H19-induced cardiomyocyte autophagy involves the PI3K/Akt/mTOR signaling pathway, the current research team injected 3-MA into the culture medium of cardiomyocytes. Interestingly, 3-MA significantly reversed the H19-induced increases of

mTOR, p-mTOR, p-PI3K and p-Akt, indicating that H19 is involved in high glucose-induced autophagy by regulating the PI3K/Akt/mTOR signaling pathway.However, in this study, we lack studies on the effects of SJTYD on other animal models of diabetes to verify its role.

CONCLUSIONS

The current study found that SJTYD can protect against DCM by inhibiting cardiomyocyte autophagy through the activation of lncRNA H19, reactive oxygen species (ROS), and the PI3K/Akt/mTOR signaling pathway. SJTYD may be an effective strategy to ameliorate diabetic myocardial injuries.

AUTHORS' DISCLOSURE STATEMENT

Grants from the National Natural Science Foundation of China (Grant No.81703894 to MJS) supported the study. All authors declare that they have no conflicts of interest related to the study.

REFERENCE

1. Bao PP, Zhao ZG, Gao YT, et al. Association of type 2 diabetes genetic variants with breast cancer survival among Chinese women. *PLoS One*. 2015;10(2):e0117419. doi:10.1371/journal.pone.0117419
2. Chengji W, Xianjin F. Exercise protects against diabetic cardiomyopathy by the inhibition of the endoplasmic reticulum stress pathway in rats. *J Cell Physiol*. 2019;234(2):1682-1688. doi:10.1002/jcp.27038
3. Mahalakshmi A, Kurian GA. Evaluating the impact of diabetes and diabetic cardiomyopathy rat heart on the outcome of ischemia-reperfusion associated oxidative stress. *Free Radic Biol Med*. 2018;118:35-43. doi:10.1016/j.freeradbiomed.2018.02.021
4. Liu Z, Zhang Y, Tang Z, et al. Matrine attenuates cardiac fibrosis by affecting ATF6 signaling pathway in diabetic cardiomyopathy. *Eur J Pharmacol*. 2017;804:21-30. doi:10.1016/j.ejphar.2017.03.061
5. Huynh K, Bernardo BC, McMullen JR, Ritchie RH. Diabetic cardiomyopathy: mechanisms and new treatment strategies targeting antioxidant signaling pathways. *Pharmacol Ther*. 2014;142(3):375-415. doi:10.1016/j.pharmthera.2014.01.003
6. Filomeni G, De Zio D, Cecconi F. Oxidative stress and autophagy: the clash between damage and metabolic needs. *Cell Death Differ*. 2015;22(3):377-388. doi:10.1038/cdd.2014.150
7. Zhang C, Yu H, Yang H, Liu B. Activation of PI3K/PKB/GSK-3β signaling by sciadopitysin protects cardiomyocytes against high glucose-induced oxidative stress and apoptosis. *J Biochem Mol Toxicol*. 2021;35(10):e22887. doi:10.1002/jbt.22887
8. Tang Z, Wang P, Dong C, Zhang J, Wang X, Pei H. Oxidative Stress Signaling Mediated Pathogenesis of Diabetic Cardiomyopathy. *Oxid Med Cell Longev*. 2022;2022:5913374. doi:10.1155/2022/5913374
9. Li Z, Dou P, Liu T, He S. *Application of Long Noncoding RNAs in Osteosarcoma: Biomarkers and Therapeutic Targets.* Cellular Physiology & Biochemistry International Journal of Experimental Cellular Physiology Biochemistry & Pharmacology; 2017:1407-1419.
10. Lorenzen JM, Thum T. Long noncoding RNAs in kidney and cardiovascular diseases. *Nat Rev Nephrol*. 2016;12(6):360-373. doi:10.1038/nrneph.2016.51
11. Yu D, Tang C, Liu P, Qian W, Sheng L. Withdrawal Notice: Targeting lncRNAs for Cardiovascular Therapeutics in Coronary Artery Disease. *Curr Pharm Des*. 2018;24. doi:10.2174/1381612824666180108120727
12. Yoshimura H, Matsuda Y, Yamamoto M, Kamiya S, Ishiwata T. Expression and role of long non-coding RNA H19 in carcinogenesis. *Front Biosci (Landmark Ed)*. 2018;23(4):614-625.
13. Gabory A, Ripoche M-A, Yoshimizu T, Dandolo L. The H19 gene: regulation and function of a non-coding RNA. *Cytogenet Genome Res*. 2006;113(1-4):188-193. doi:10.1159/000090831
14. Geng H, Bu HF, Liu F, et al. In Inflamed Intestinal Tissues and Epithelial Cells, Interleukin 22 Signaling Increases Expression of H19 Long Noncoding RNA, Which Promotes Mucosal Regeneration. *Gastroenterology*. 2018;155(1):144-155. doi:10.1053/j.gastro.2018.03.058
15. Liu L, An X, Li Z, et al. The H19 long noncoding RNA is a novel negative regulator of cardiomyocyte hypertrophy. *Cardiovasc Res*. 2016;111(1):56-65. doi:10.1093/cvr/cvw078
16. Wu X, Wu Y, Wang Z, et al. A Cascade-Targeting Nanocapsule for Enhanced Photothermal Tumor Therapy with Aid of Autophagy Inhibition. *Adv Healthc Mater*. 2018;7(11):e1800121. doi:10.1002/adhm.201800121
17. Metaxakis A, Ploumi C, Tavernarakis N. Autophagy in Age-Associated Neurodegeneration. *Cells*. 2018;7(5):37. doi:10.3390/cells7050037
18. Wang F, Jia J, Rodrigues B. Autophagy, Metabolic Disease, and Pathogenesis of Heart Dysfunction. *Can J Cardiol*. 2017;33(7):850-859. doi:10.1016/j.cjca.2017.01.002
19. Jafari M, Ghadami E, Dadkhah T, Akhavan-Niaki H. PI3k/AKT signaling pathway: erythropoiesis and beyond. *J Cell Physiol*. 2019;234(3):2373-2385. doi:10.1002/jcp.27262
20. Yun HR, Jo YH, Kim J, Shin Y, Kim SS, Choi TG. Roles of Autophagy in Oxidative Stress. *Int J Mol Sci*. 2020;21(9):3289. doi:10.3390/ijms21093289
21. Mehrzadi S, Pourhanifeh MH, Mirzaei A, Moradian F, Hosseinzadeh A. An updated review of mechanistic potentials of melatonin against cancer: pivotal roles in angiogenesis, apoptosis, autophagy, endoplasmic reticulum stress and oxidative stress. *Cancer Cell Int*. 2021;21(1):188. doi:10.1186/s12935-021-01892-1
22. Muriach M, Flores-Bellver M, Romero FJ, Barcia JM. Diabetes and the brain: oxidative stress, inflammation, and autophagy. *Oxid Med Cell Longev*. 2014;2014:102158. doi:10.1155/2014/102158
23. Tao Z, Feng C, Mao C, et al. MiR-4465 directly targets PTEN to inhibit AKT/mTOR pathway-mediated autophagy. *Cell Stress Chaperones*. 2019;24(1):105-113. doi:10.1007/s12192-018-0946-6
24. Shiau JP, Chuang YT, Cheng YB, et al. Impacts of Oxidative Stress and PI3K/AKT/mTOR on Metabolism and the Future Direction of Investigating Fucoidan-Modulated Metabolism. *Antioxidants*. 2022;11(5):911. doi:10.3390/antiox11050911
25. Zhang ZY, Bao XL, Cong YY, Fan B, Li GY. Autophagy in Age-Related Macular Degeneration: A Regulatory Mechanism of Oxidative Stress. *Oxid Med Cell Longev*. 2020;2020:2896036. doi:10.1155/2020/2896036
26. Wang Y, Xu W, Yan Z, et al. Metformin induces autophagy and G0/G1 phase cell cycle arrest in myeloma by targeting the AMPK/mTORC1 and mTORC2 pathways. *J Exp Clin Cancer Res*. 2018;37(1):63. doi:10.1186/s13046-018-0731-5
27. He D, Sun X, Yang H, Li X, Yang D. TOFA induces cell cycle arrest and apoptosis in ACHN and 786-O cells through inhibiting PI3K/Akt/mTOR pathway. *J Cancer*. 2018;9(15):2734-2742. doi:10.7150/jca.26374
28. Filomeni G, De Zio D, Cecconi F. Oxidative stress and autophagy: the clash between damage and metabolic needs. *Cell Death Differ*. 2015;22(3):377-388. doi:10.1038/cdd.2014.150
29. Gurusamy N, Das DK. Autophagy, redox signaling, and ventricular remodeling. *Antioxid Redox Signal*. 2009;11(8):1975-1988. doi:10.1089/ars.2009.2524
30. Lü M, Wang TY, Tian XX, et al. [Interaction of anti-thrombotic and anti-inflammatory activities of commonly used traditional Chinese medicine for promoting blood circulation and removing blood stasis revealed by network pharmacology analysis]. *Yao Xue Xue Bao*. 2015;50(9):1135-1141.
31. Ouyang LD, Hu XS, Niu M, et al. [Mechanisms of Hirudo in promoting blood circulation and removing stasis based on network pharmacology]. *Zhongguo Zhongyao Zazhi*. 2018;43(9):1901-1906.
32. Jing WU, Ying-Dong LU, Yuan GZ, et al. Effects of Shengjie Tongyu Decoction on pulmonary vascular and right ventricular remodeling in rat model of pulmonary arterial hypertension induced by monocrotaline. *Zhonghua Zhongyiyao Zazhi*. 2019.
33. Chen M, Cheng W, Shi Z, et al. Shengjie Tongyu Granule Inhibits Vascular Remodeling in ApoE-Gene-Knockout Mice. *Evid Based Complement Alternat Med*. 2012;2012:897875. doi:10.1155/2012/897875
34. Zhai G, Dong J, Wang S, Shang K. Clinical research on shengjie tongyu granules in the treatment of meteorological cardiovascular disease. *Pak J Pharm Sci*. 2015;28(2)(suppl):785-789.
35. Ma CY, Ma YQ, Deng M. Mechanism of Zhen Wu Decoction in the Treatment of Heart Failure Based on Network Pharmacology and Molecular Docking. *Evid Based Complement Alternat Med*. 2022;2022:4877920. doi:10.1155/2022/7723358
36. Thomas AA, Biswas S, Feng B, Chen S, Gonder J, Chakrabarti S. lncRNA H19 prevents endothelial-mesenchymal transition in diabetic retinopathy. *Diabetologia*. 2019;62(3):517-530. doi:10.1007/s00125-018-4797-6
37. Dobin A, Davis CA, Schlesinger F, et al. STAR: ultrafast universal RNA-seq aligner. *Bioinformatics*. 2013;29(1):15-21. doi:10.1093/bioinformatics/bts635
38. Li B, Dewey CN. RSEM: accurate transcript quantification from RNA-Seq data with or without a reference genome. *BMC Bioinformatics*. 2011;12(1):323. doi:10.1186/1471-2105-12-323
39. Robinson MD, McCarthy DJ, Smyth GK. edgeR: a Bioconductor package for differential expression analysis of digital gene expression data. *Bioinformatics*. 2010;26(1):139-140. doi:10.1093/bioinformatics/btp616
40. Chen S, Zhou Y, Chen Y, Gu J. fastp: an ultra-fast all-in-one FASTQ preprocessor. *Bioinformatics*. 2018;34(17):i884-i890. doi:10.1093/bioinformatics/bty560
41. Chen L, Zhang YH, Wang S, Zhang Y, Huang T, Cai YD. Prediction and analysis of essential genes using the enrichments of gene ontology and KEGG pathways. *PLoS One*. 2017;12(9):e0184129. doi:10.1371/journal.pone.0184129
42. Glick D, Barth S, Macleod KF. Autophagy: cellular and molecular mechanisms. *J Pathol*. 2010;221(1):3-12. doi:10.1002/path.2697